China Economic Review 94 (2025) 102517

Contents lists available at ScienceDirect

China Economic Review

journal homepage: www.elsevier.com/locate/chieco

The time-varying zone-like and asymmetric preference of central banks: Evidence from China ☆

Chuanglian Chen [a], Xiaobin Liu [b,*], Jun Yu [c], Tao Zeng [d]

[a] Institute of Finance and School of Economics, Jinan University, China
[b] Lingnan College, Sun Yat-sen University, China
[c] Faculty of Business Administration and APAEM, University of Macau, Macao, China
[d] School of Economics, Academy of Financial Research, Beijing Research Center, Zhejiang University, China

ARTICLE INFO

JEL classification:
E5
C32
C51
C52
E52
E58

Keywords:
Time-varying parameter model
Forward-looking monetary policy rule
Leverage
Asymmetric and zone-like preference

ABSTRACT

This paper develops a framework to investigate the time-varying asymmetric and zone-like preferences of a central bank. We derive the optimal forward-looking monetary policy rule and explore four distinct types of loss related to inflation, output, and leverage, resulting in 64 distinct models. We estimate these models and utilize the Akaike information criterion (AIC) to select the most suitable one. Using data from 1996 to 2022, we find that the People's Bank of China (PBoC): (1) reacts to inflation gaps with slight asymmetry, featuring a no-intervention zone between -1% and 1%; (2) intervenes asymmetrically in output gaps, displaying stronger inclination toward averting overheating than downturns; (3) applies symmetric regulation to leverage gaps. These findings underscore the PBoC's adaptability and responsiveness to economic fluctuations and its preference for risk management.

1. Introduction

Understanding monetary policy targets and central banks' corresponding reactions is fundamental to monetary economics. This paper develops a comprehensive framework for analyzing central banks' time-varying preferences and their implications for monetary policy rules. Based on this framework, we examine the asymmetric and "zone-like" characteristics of the People's Bank of China (PBoC) and their implications for the monetary policy rule, and investigate leverage's role within China's multi-objective policy framework.

Central banks continuously adjust their policy targets in response to changing economic conditions. Following the subprime crisis, their focus expanded beyond traditional growth and inflation objectives to include financial risks. During the COVID-19 pandemic, China implemented expansionary fiscal and monetary policies to stimulate recovery, increasing its leverage ratio by 12.5% by December 2022 compared to pre-pandemic levels. While credit expansion can support economic growth, excessive leverage

☆ Chen acknowledges the financial support from the National Natural Science Foundation of China (No. 72071094), Natural Science Foundation of Guangdong, China (No. 2024A1515012673), Technology Elite Navigation Project of Guangzhou, China (No. 2024A04J6373), Basic Project of Guangdong Financial Society, China, (No. JCKT202407) and Fundamental Research Funds for Central Universities, China. Liu acknowledges the financial support from the National Natural Science Foundation of China (No. 72473164, No. 72003171). Yu gratefully acknowledges the financial support from UMDF and APAEM. Zeng gratefully acknowledges the financial support from the National Natural Science Foundation of China (No. 72073121, 72141305) and the National Social Science Fund of China (No. 24&ZD070). All errors are our own.

* Corresponding author.
E-mail addresses: chenchuanglian@jnu.edu.cn (C. Chen), liuxb53@mail.sysu.edu.cn (X. Liu), junyu@um.edu.mo (J. Yu), tzeng@zju.edu.cn (T. Zeng).

https://doi.org/10.1016/j.chieco.2025.102517
Received 4 December 2024; Received in revised form 15 July 2025; Accepted 21 July 2025
Available online 30 July 2025

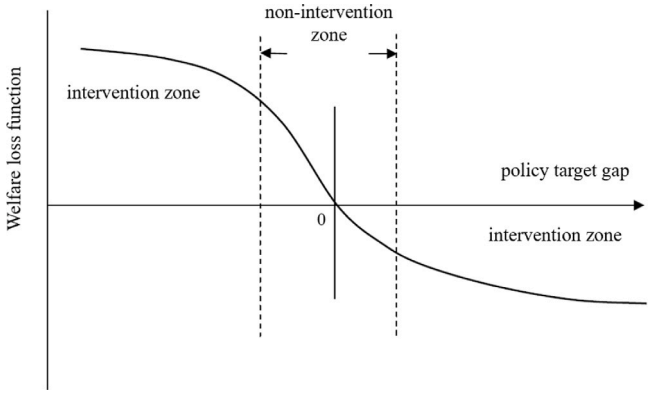

Fig. 1. The loss function with asymmetrical and zone-like properties.

heightens financial system vulnerability and increases crisis risk. Consequently, the PBoC faces the complex challenge of balancing financial stability with sustainable growth.

Conventional monetary policy rules typically prescribe linear responses to economic deviations, corresponding to quadratic loss functions in central bank preferences. However, central banks often exhibit asymmetric preferences when managing multiple objectives, potentially prioritizing the avoidance of deflation over inflation or vice versa. Furthermore, central banks may maintain a "no-intervention zone", allowing market self-regulation for minor deviations while intervening only during significant disruptions, as illustrated in Fig. 1. This balance between regulatory intervention and market adjustment is essential for sustainable economic growth. Beyond these asymmetric and zone-like preferences, central banks' policy stances continuously adapt to evolving economic conditions.

Our paper examines the PBoC's behavior, focusing specifically on the evolution of its asymmetric and zone-like preferences in managing multiple policy targets. We extend the central bank's loss function by allowing weights assigned to different policy objectives to vary temporally. The central bank minimizes these time-varying losses to derive an optimal forward-looking monetary policy rule characterized by time-varying parameters (TVP).[1]

Specifically, we analyze the PBoC's approach to inflation regulation, output stabilization, and macro-leverage management. By assigning different parameters to each policy objective, we explore four types of loss functions: quadratic, asymmetric, symmetrically inert, and asymmetrically inert. This approach yields 64 distinct models characterizing the PBoC's preferences and monetary policy rules. The most sophisticated response function exhibits time-varying behavior with both inertia and asymmetry, integrating all previously identified characteristics. Following Riboni and Ruge-Murcia (2023), we employ the Akaike information criterion (AIC) to select the model that best captures the PBoC's behavior.

Our framework enhances understanding of the PBoC's time-varying zone-like and asymmetric preferences. Empirical analysis reveals that the PBoC demonstrates notable inertia with a slightly asymmetrical pattern in its response to inflation gaps. The central bank exhibits asymmetric behavior in both its loss function and response to output gaps, while maintaining a quadratic loss function and linear response to leverage gaps. These time-varying interest rate adjustments provide compelling evidence of the central bank's evolving strategic approach to economic transformations.

Further examination of time-varying policy reactions yields three key insights. First, the PBoC adopts an inertial approach to inflation, intervening only when inflation deviates by more than 1% from its target. Within this"inert zone" (−1%, 1%), the central bank refrains from intervention, allowing market self-regulation. The PBoC exhibits slightly greater concern for excessive inflation than for deflation, as its asymmetric responses demonstrate: a 1% increase above target triggers an interest rate increase of 0.05% to 0.3%, while a 1% decrease prompts a reduction of 0.04% to 0.3%. Since late 2020, influenced by the COVID-19 pandemic, the PBoC's counter-cyclical measures have become more moderate, indicating a cautious monetary policy approach with clearly defined boundaries for inflation regulation.

Second, the PBoC demonstrates stronger aversion to economic overheating than to recession. Since early 2020, due to COVID-19, the central bank's policy stance has shifted significantly, with losses occasionally transforming into gains. Prior to 2020, monetary policy operated predominantly counter-cyclical but subsequently adopted a pro-cyclical orientation. Unlike its approach to inflation, the PBoC maintains no "inertia zone" for output gaps, applying greater regulatory force to curb positive output gaps than negative ones of equal magnitude. This asymmetric approach suggests that China prioritizes stable economic growth over strict economic cycle regulation.

Third, the PBoC employs a balanced regulatory approach to leverage gaps, intervening equally regardless of whether leverage rises or falls. Before 2005, monetary policies did not explicitly target leverage, with minimal and occasionally counterproductive

[1] The TVP model effectively detects broad, potentially enduring changes in individual parameters, providing smooth estimates of discrete changes and facilitating the assessment of policy dynamics. It offers a parsimonious approximation for multiple policy shifts without requiring numerous parameter and break date estimations, making it a flexible and tractable method for uncovering temporal variations in policy response functions (Boivin, 2006).

responses. Since 2005, however, there has been a significant shift toward managing credit growth, evidenced by increased policy focus and intervention intensity. This strategic evolution is reflected in rising time-varying losses and more active policy measures targeting leverage.

Related literature

This paper contributes to three strands of literature. First, it advances the discourse on modeling monetary policy rule responses. Taylor (1993)'s seminal work advocates linear interest rate adjustments driven by inflation and output gaps. However, researchers like Castro (2011) argue that this framework fails to capture the complexities of real-world monetary policy implementation. Studies by Baele, Bekaert, Cho, Inghelbrecht, and Moreno (2015) and Nakajima and West (2013) highlight significant shifts in monetary policy response functions as interest rates approach the zero lower bound. Additionally, Benigno and Rossi (2021), Robert Nobay and Peel (2003), Ruge-Murcia (2003), and Surico (2007) examine asymmetric responses in monetary policy reaction functions. Central banks' risk aversion varies under different economic conditions, necessitating monetary policy rules with time-varying parameters as demonstrated by Boivin (2006), Cogley and Sargent (2005), Filardo, Hubert, and Rungcharoenkitkul (2022), and Kim and Nelson (2006). These evolving studies highlight monetary policy's dynamic nature and the necessity for continual refinement to address changing economic conditions. Our paper makes a distinct contribution by examining monetary policy rules embedded in the time-varying, zone-like, and asymmetric preferences of central banks.

Second, our study contributes to literature on the loss functions and preferences of central banks. Understanding these preferences is crucial for interpreting monetary policy decisions. Shapiro and Wilson (2022) introduces an innovative preference estimation approach using sentiment data, while Riboni and Ruge-Murcia (2023) models central bank decision processes. Several studies directly model central bank loss functions, often suggesting asymmetric specifications to better capture preferences (Robert Nobay & Peel, 2003; Ruge-Murcia, 2003; Surico, 2007), resulting in nonlinear response functions. Orphanides and Wieland (2000) proposes a "region loss function" to capture zone-like central bank behavior, and Boinet and Martin (2008) demonstrates the existence of zone properties in inflation targeting. These works highlight traditional quadratic loss functions' limitations in capturing central bank preferences' nuances, emphasizing nonlinear Taylor rules and policy asymmetries. We extend central banks' loss functions by incorporating time-varying policy target weights, enabling formulation of an optimal time-varying parameter forward-looking monetary policy rule. Our approach also nests with second-order approximations of utility-based welfare functions in New-Keynesian models, aligning with work by Benigno and Rossi (2021), Giannoni and Woodford (2017), and Gross and Hansen (2021).

Third, our research contributes to literature examining optimal monetary policy responses to multiple policy objectives. Recent studies have expanded monetary policy rules to include additional considerations, such as financial imbalances (Filardo et al., 2022), asset prices (Gambacorta & Signoretti, 2014), and exchange rates (Bruno & Shin, 2015). Leverage targets have gained increasing importance in monetary policy, particularly following financial and European debt crises, as elevated global debt levels contribute to low-interest-rate environments (Adrian, Boyarchenko, & Giannone, 2019; Blanchard, 2019; Gourinchas & Rey, 2019) and exacerbate economic inequality (Auclert, 2019; Bartscher, Kuhn, Schularick, & Steins, 2020). Recognizing leverage's significance in monetary policy frameworks, it is essential to investigate its role as a policy objective (Chen & Dai, 2018; Dong, Xu, & Tan, 2021). Silvo (2019) demonstrates that an extended DSGE model incorporating inflation and banking sector leverage can effectively regulate cyclical fluctuations. Building on these insights, our study incorporates credit leverage gaps into the central bank loss function, enhancing the expanded monetary policy rule's applicability and realism. This approach is particularly relevant for China's high-leverage economy and the PBoC's need to coordinate multiple policy objectives.

This paper is organized as follows: Section 2 derives the optimal monetary policy rule embedded in the central bank's loss function with time-varying weights and examines its policy implications. Section 3 presents our estimation strategy and model selection criteria. Section 4 describes the dataset employed in our analysis. Section 5 presents the empirical results and their interpretation, including a comparative analysis between the optimal model and alternative specifications. Section 6 concludes with key findings and implications.

2. The model

2.1. Preference of the central bank

We extend the loss function proposed by Boinet and Martin (2008), Robert Nobay and Peel (2003), Ruge-Murcia (2003), and Surico (2007) to incorporate time-varying weights that reflect the monetary authority's evolving preferences. We consider inertial or zone-like behavior and asymmetry in policy responses. The resulting loss function at time t is

$$L_t = \left\{ \begin{array}{c} \frac{1}{\gamma_\pi^2 \kappa_\pi} \left[e^{\gamma_\pi \left(\pi_t - \pi_t^*\right)^{\kappa_\pi}} - \gamma_\pi \left(\pi_t - \pi_t^*\right)^{\kappa_\pi} - 1 \right] + \frac{\tilde{w}_{y,t}}{\gamma_y^2 \kappa_y} \left[e^{\gamma_y y_t^{\kappa_y}} - \gamma_y y_t^{\kappa_y} - 1 \right] \\ + \frac{\tilde{w}_{l,t}}{\gamma_l^2 \kappa_l} \left[e^{\gamma_l l_t^{\kappa_l}} - \gamma_l l_t^{\kappa_l} - 1 \right] + \frac{1}{2} \tilde{w}_{i,t} \left(i_t - i_t^*\right)^2 \end{array} \right\}, \tag{1}$$

where π_t^* represents the inflation target, and $\pi_t - \pi_t^*$ denotes the inflation gap. The output gap is y_t, and l_t represents the leverage gap. The nominal interest rate is i_t, and the equilibrium interest rate is denoted as i^*. The weights $\tilde{w}_{y,t}$, $\tilde{w}_{l,t}$, and $\tilde{w}_{i,t}$ are relative, time-varying, and independent of the variables $\left(\pi_t - \pi_t^*\right)$, y_t, and l_t. The parameters γ_π, γ_y, γ_l, κ_π, κ_y, and κ_l characterize the central bank's preferences. Specifically, κ_π, κ_y, and κ_l capture the asymmetry and zone-like properties of the loss function, while γ_π, γ_y, and γ_l determine the slope of the loss function and the direction of asymmetry.

The loss function in Eq. (1) mirrors established central bank regulatory practices. The monetary policy rule comprises two essential components confirmed by empirical evidence and theoretical frameworks (Kim & Nelson, 2006; Taylor, 1993; Woodford & Walsh, 2005). The first component ensures interest rate stability through policy rule smoothness, while the second adjusts rates to achieve multiple policy objectives. Stronger weighting of either component reflects the central bank's relative preference for stability versus target achievement. In theoretical frameworks, this second component functions as the target or optimal interest rate, which we incorporate into our preference function as the final term in Eq. (1). Following Surico (2007), we adopt a quadratic specification for the interest rate gap, which assumes symmetric costs for deviations from the target rate. This term lacks asymmetry because it serves specifically as the target interest rate for regulating policy objectives rather than requiring an asymmetric form. We deliberately included this component to ensure both target interest rate and smoothness are properly integrated into the Taylor rule model for subsequent analysis.[2]

Furthermore, the specification is general, with its form dependent on parameter values. When $\tilde{w}_{y,t}$, $\tilde{w}_{l,t}$, and $\tilde{w}_{i,t}$ are constant and $\gamma_\pi \to 0$, $\gamma_y \to 0$, $\gamma_l \to 0$, $\kappa_\pi = \kappa_y = \kappa_l = 1$, the function reduces to a quadratic loss function with linear responses to deviations. When relative weights remain constant over time, the simplified loss function becomes $\frac{1}{2}\left[\left(\pi_t - \pi_t^*\right)^2 + \tilde{w}_y y_t^2 + \tilde{w}_l l_t^2 + \tilde{w}_i \left(i_t - i_t^*\right)^2\right]$, which can be derived as a second-order approximation of the utility-based welfare function within a New-Keynesian business cycle model, as Giannoni and Woodford (2017) and Woodford and Walsh (2005) demonstrate. Therefore, any observed asymmetry in the central bank's objectives may indicate asymmetry in the representative agent's utility function, suggesting that our framework captures welfare impacts of business cycle fluctuations beyond second-order approximations.

The generalized loss function accommodates asymmetry, with the degree captured by the γ parameters. When $\gamma_\pi > 0$, policymakers experience greater loss when inflation exceeds the target compared to when it falls below by the same magnitude. This concept has been examined in several studies, including Robert Nobay and Peel (2003), Ruge-Murcia (2003), and Surico (2007).

The loss function exhibits zone-like behavior for a policy target when its associated parameter, κ, exceeds one. This preference is particularly relevant for inflation target zones, as Orphanides and Wieland (2000) initially introduced. In scenarios with zone-like preferences, policymakers remain indifferent to inflation rates within a specified range where the marginal loss is zero. The width of this zone expands as κ_π increases. The slope of the loss function, which determines the magnitude of marginal loss both within and outside the zone, is influenced by the parameter γ_π.

When κ_π is even, both the indifference zone and the loss from inflation deviations outside this zone are symmetric. When κ_π is odd, both the zone and the associated loss become asymmetric. Specifically, when $\gamma_\pi > 0$, greater loss is incurred for positive inflation gaps. Appendix A provides a comprehensive overview of various loss function specifications.

2.2. The monetary policy rule

To analyze the central bank's behavior and its response to different economic variables under various loss functions, we adopt the monetary policy framework from Bianchi, Lettau, and Ludvigson (2022). The IS curve describes the relationship between output gaps and nominal interest rates, while the Phillips curve relates inflation gaps to output gaps and expected inflation.

$$y_t = \theta_0 - \theta_1 \left(i_t - \mathbb{E}_t\left[\pi_{t+1}\right]\right) + \mathbb{E}_t\left[y_{t+1}\right] + \varepsilon_t, \tag{2}$$

where $\theta_1 \in (0, 1)$ is the adjustment coefficient of the output gap to the interest rate, and ε_t is the i.i.d. demand shock with mean 0 and variance σ_ε^2.

The New Keynesian Phillips curve is:

$$\pi_t - \pi_t^* = \eta_0 + \eta_1 \mathbb{E}_t\left[\pi_{t+1} - \pi_{t+1}^*\right] + \lambda y_t + \upsilon_t, \tag{3}$$

where $\eta_1 \in (0, 1)$ is the inflation smoothing coefficient, λ is the adjustment coefficient of inflation to the output gap, and υ_t is the i.i.d supply shock with mean 0 and variance σ_υ^2.

The credit leverage gap, often proxied by the Credit-to-GDP gap, is also known as the Cyclically Adjusted Credit-to-GDP Ratio (CAC). It measures the difference between the credit-to-GDP ratio and its long-term trend, estimated using the Hodrick–Prescott (HP) filter. The Bank for International Settlements has shown that setting an early warning threshold at 10% can predict approximately 66.67% of global banking crises since the 1970s (Drehmann & Tsatsaronis, 2014). Following Bruno and Shin (2015), Chen and Dai (2018), and Dong et al. (2021), since the leverage gap is positively correlated with the real interest rate and the output gap, we model the evolution of the credit leverage gap as:

$$l_t = k_0 - k_1 \left(i_t - \mathbb{E}_t\left[\pi_{t+1}\right]\right) + k_2 y_t + \zeta_t, \tag{4}$$

where the credit leverage gap l_t, first introduced by Borio and Lowe (2002), is defined as the difference between the Credit-to-GDP Ratio and its long-term trend, estimated using the HP filter. The coefficient $k_1 \in (0, 1)$ represents the adjustment of credit leverage to the interest rate, meaning that a larger coefficient results in a greater counter-cyclical effect of the interest rate on the credit leverage gap. The coefficient $k_2 > 0$ captures the dynamic relationship between the business cycle and the credit leverage gap,

[2] This simplification abstracts from general equilibrium effects where asymmetries in inflation or output preferences could extend to the interest rate itself, creating asymmetric costs for raising versus lowering rates. Incorporating such effects would require a non-quadratic specification for the interest rate loss term, which is a promising direction for future research.

indicating that credit scale increases as the economy expands, resulting in an increase in the credit leverage gap. The i.i.d. leverage risk shock ζ_t has a mean of 0 and variance σ_ζ^2.

The central bank minimizes loss by adjusting a basket of monetary policy tools, while considering the constraints imposed by the IS curve and the Phillips curve. Since the central bank must make policy decisions before the realization of economic shocks and the determination of variables within the system, it sets a nominal interest rate that accounts for the dynamics of the economic system:

$$\min_{\{i_t\}} \mathbb{E}_{t-1}\left[\sum_{\tau=0}^{\infty}\delta^\tau L_{t+\tau}\right], \tag{5}$$

where δ is the discount factor and L_t is defined in Eq. (1). The central bank solves the minimization problem by setting the first partial derivative of (5) with respect to i_t equal to 0, which yields an optimal interest rate that satisfies:

$$\mathbb{E}_{t-1}\left[\frac{\partial L_t}{\partial i_t}+\sum_{\tau=1}\delta^\tau\frac{\partial L_{t+\tau}}{\partial i_t}\right]=0.$$

This first-order condition allows us to obtain the optimal interest rate:

$$\begin{aligned}\hat{i}_t =&\omega_{0,t}+\omega_{y,t}\mathbb{E}_t\left[\mathcal{G}\left(y_{t+1};\kappa_y,\gamma_y\right)y_{t+1}\right]+\omega_{l,t}\mathbb{E}_t\left[\mathcal{G}\left(l_{t+1};\kappa_l,\gamma_l\right)l_{t+1}\right]\\&+\omega_{\pi,t}\mathbb{E}_t\left[\mathcal{G}\left(\pi_{t+1}-\pi^*_{t+1};\kappa_\pi,\gamma_\pi\right)\left(\pi_{t+1}-\pi^*_{t+1}\right)\right],\end{aligned} \tag{6}$$

where $\mathcal{G}(x;\kappa,\gamma)=\frac{x^{\kappa-2}\left(e^{\gamma x^\kappa}-1\right)}{\gamma}$, $\omega_{0,t}=\mathbb{E}_t\left[i^*_{t+1}\right]$, $\omega_{y,t}=\mathbb{E}_t\left[\frac{\tilde{w}_{y,t+1}\theta_1}{\tilde{w}_{i,t+1}}\right]$, $\omega_{l,t}=\mathbb{E}_t\left[\frac{\tilde{w}_{l,t+1}(k_1+\theta_1k_2)}{\tilde{w}_{i,t+1}}\right]$, $\omega_{\pi,t}=\mathbb{E}_t\left[\frac{\lambda\theta_1}{\tilde{w}_{i,t+1}}\right]$, and $\hat{i}_t=\mathbb{E}_t\left[i_{t+1}\right]$. The derivation is given in Appendix B. According to the Taylor expansion around $\gamma_\pi=\gamma_y=\gamma_l=0$, we can approximate Eq. (6) as

$$\begin{aligned}\hat{i}_t \approx&\omega_{0,t}+\omega_{y,t}\mathbb{E}_t\left[y_{t+1}^{2\kappa_y-1}\left(1+\frac{\gamma_y}{2}y_{t+1}^{\kappa_y}\right)\right]+\omega_{l,t}\mathbb{E}_t\left[l_{t+1}^{2\kappa_l-1}\left(1+\frac{\gamma_l}{2}l_{t+1}^{\kappa_l}\right)\right]\\&+\omega_{\pi,t}\mathbb{E}_t\left[\left(\left(\pi_{t+1}-\pi^*_{t+1}\right)^{2\kappa_\pi-1}\left(1+\frac{\gamma_\pi}{2}\left(\pi_{t+1}-\pi^*_{t+1}\right)^{\kappa_\pi}\right)\right)\right].\end{aligned} \tag{7}$$

To account for the interest rate smoothing property documented in the literature, we assume that the central bank adjusts the interest rate according to:

$$\begin{aligned}i_{t+1} =&\omega_{0,t}+\omega_{y,t}\mathbb{E}_t\left[y_{t+1}^{2\kappa_y-1}\left(1+\frac{\gamma_y}{2}y_{t+1}^{\kappa_y}\right)\right]+\omega_{l,t}\mathbb{E}_t\left[l_{t+1}^{2\kappa_l-1}\left(1+\frac{\gamma_l}{2}l_{t+1}^{\kappa_l}\right)\right]\\&+\omega_{\pi,t}\mathbb{E}_t\left[\left(\left(\pi_{t+1}-\pi^*_{t+1}\right)^{2\kappa_\pi-1}\left(1+\frac{\gamma_\pi}{2}\left(\pi_{t+1}-\pi^*_{t+1}\right)^{\kappa_\pi}\right)\right)\right]+\rho_t i_t+e_{t+1}.\end{aligned} \tag{8}$$

where ρ_t is the smoothing parameter and e_{t+1} is the monetary policy shock, which captures unanticipated changes in the interest rate that cannot be explained by the systematic response to macroeconomic variables.

When $\kappa_\pi=\kappa_y=\kappa_l=1$ and $\gamma_\pi=\gamma_y=\gamma_l=0$, the monetary policy in Eq. (8) simplifies to the widely-used linear forward-looking monetary policy rule as in (Boivin, 2006; Taylor, 1993):

$$i_{t+1}=\omega_{0,t}+\omega_{\pi,t}\mathbb{E}_t\left[\pi_{t+1}-\pi^*_{t+1}\right]+\omega_{y,t}\mathbb{E}_t\left[y_{t+1}\right]+\omega_{l,t}\mathbb{E}_t\left[l_{t+1}\right]+\rho_t i_t+e_{t+1}. \tag{9}$$

Our model in Eq. (8) thus offers a more general framework. As discussed in Section 2.1, this model can identify the central bank's preferences and capture monetary policy characteristics, such as symmetric or zone-like preferences.

Following Primiceri (2005), to estimate the autoregression coefficient, we apply the following transformation:

$$\rho_t=\frac{1}{1+e^{-\tilde{\rho}_t}}. \tag{10}$$

We rewrite the model and specify the evolution of time-varying parameters as:

$$\begin{aligned}i_{t+1} =&\omega_{0,t}+\omega_{y,t}\left(y_{t+1}^{2\kappa_y-1}+\frac{\gamma_y}{2}y_{t+1}^{3\kappa_y-1}\right)+\omega_{l,t}\left(l_{t+1}^{2\kappa_l-1}+\frac{\gamma_l}{2}l_{t+1}^{3\kappa_l-1}\right)\\&+\omega_{\pi,t}\left(\left(\pi_{t+1}-\pi^*_{t+1}\right)^{2\kappa_\pi-1}+\frac{\gamma_\pi}{2}\left(\pi_{t+1}-\pi^*_{t+1}\right)^{3\kappa_\pi-1}\right)+\rho_t i_t+\xi_t,\end{aligned} \tag{11}$$

$$\boldsymbol{\beta}_t=\boldsymbol{\beta}_{t-1}+\varpi_t,\ \varpi_t\sim N(0,\boldsymbol{\Sigma}), \tag{12}$$

where $\boldsymbol{\beta}_t=\left(\omega_{0,t},\omega_{y,t},\omega_{l,t},\omega_{\pi,t},\tilde{\rho}_t\right)'$, $\boldsymbol{\Sigma}=diag\left(\sigma_0^2,\sigma_y^2,\sigma_l^2,\sigma_\pi^2,\sigma_\rho^2\right)$, ϖ_t and ξ_t are mutually independent, and

$$\begin{aligned}\xi_t =&\omega_{y,t}\left(\mathbb{E}_t\left[y_{t+1}^{2\kappa_y-1}\left(1+\frac{\gamma_y}{2}y_{t+1}^{\kappa_y}\right)\right]-y_{t+1}^{2\kappa_y-1}\left(1+\frac{\gamma_y}{2}y_{t+1}^{\kappa_y}\right)\right)\\&+\omega_{l,t}\left(\mathbb{E}_t\left[l_{t+1}^{2\kappa_l-1}\left(1+\frac{\gamma_l}{2}l_{t+1}^{\kappa_l}\right)\right]-l_{t+1}^{2\kappa_l-1}\left(1+\frac{\gamma_l}{2}l_{t+1}^{\kappa_l}\right)\right)\\&+\omega_{\pi,t}\left(\mathbb{E}_t\left[\left(\pi_{t+1}-\pi^*_{t+1}\right)^{2\kappa_\pi-1}\left(1+\frac{\gamma_\pi}{2}\left(\pi_{t+1}-\pi^*_{t+1}\right)^{\kappa_\pi}\right)\right]\right.\\&\left.-\left(\pi_{t+1}-\pi^*_{t+1}\right)^{2\kappa_\pi-1}\left(1+\frac{\gamma_\pi}{2}\left(\pi_{t+1}-\pi^*_{t+1}\right)^{\kappa_\pi}\right)\right)+e_{t+1}.\end{aligned} \tag{13}$$

Sims and Zha (2001, 2006) have highlighted significant heteroscedasticity in the variance of ξ_t. To account for this, we approximate the distribution of ξ_t using a GARCH(1,1) process, following (Kim & Nelson, 2006):

$$\xi_t \left| \mathcal{I}_{t-1} \sim N\left(0, \sigma^2_{\xi,t}\right), \right. \tag{14}$$

$$\sigma^2_{\xi,t} = \alpha_0 + \alpha_1 \xi^2_{t-1} + \alpha_2 \sigma^2_{\xi,t-1}, \tag{15}$$

where $\mathcal{I}_{t-1}$ is the information set up to time $t-1$.

In this model, the parameters of interest are $\left\{\alpha_0, \alpha_1, \alpha_2, \sigma^2_0, \sigma^2_y, \sigma^2_l, \sigma^2_\pi, \sigma^2_\varrho, \gamma_\pi, \gamma_y, \gamma_l\right\}$. However, due to correlation between ξ_t and the regressors in Eq. (11), endogeneity may exist, potentially biasing the estimates. To address this issue, we employ the Heckman-type two-stage maximum likelihood estimation method described in Section 3.1, as recommended by Kim and Nelson (2006), to resolve the endogeneity problem.

3. Estimation methodology

3.1. Estimation

To address the endogeneity issue and obtain unbiased estimates, we follow Kim and Nelson (2006) and introduce instrumental variables. Using the inflation gap $\pi - \pi^*$ as an example, we specify:

$$\pi_{t+1} - \pi^*_{t+1} = Z_t \phi^\pi_t + \varepsilon^\pi_t, \tag{16}$$

$$\phi^\pi_t = \phi^\pi_{t-1} + \varpi^\pi_t, \varpi^\pi_t \sim N\left(0, \sigma^2_{\phi,\pi}\right), \varepsilon^\pi_t \sim N\left(0, \sigma^2_{\varepsilon,\pi,t}\right), \tag{17}$$

$$\sigma^2_{\varepsilon,\pi,t} = a^\pi_0 + a^\pi_1 \sigma^2_{\varepsilon,\pi,t-1} + a^\pi_2 \varepsilon^{\pi 2}_{t-1}. \tag{18}$$

The model in Eqs. (16)–(18) can be estimated via the Kalman filter. We define the instrumental variables as:

$$Z_t = \left(Z'_{t-1}, Z'_{t-2}, Z'_{t-3}, Z'_{t-4}\right)', \tilde{Z}_{t-j} = \left(i_{t-j}, \pi_{t-j} - \pi^*_{t-j}, y_{t-j}, l_{t-j}, m2_{t-j}\right)',$$

where $m2_{t-j}$ represents M2 growth. To mitigate endogeneity, we partition the regressors into predicted components and prediction errors. After applying the Kalman filter, we retain the prediction error components, denoted as $\varepsilon_{\pi,t|t-1}$. The standardized prediction errors $\varepsilon^*_{\pi,t}$ are obtained as:

$$\varepsilon_{\pi,t|t-1} = \sigma^{1/2}_{\varepsilon,\pi,t|t-1} \varepsilon^*_{\pi,t}, \varepsilon^*_t \sim N(0,1),$$

where the conditional covariance $\sigma^{1/2}_{\phi,\pi,t|t-1}$ is a by-product of the Kalman filter. We apply the same procedure for the output gap y_t and leverage gap l_t, then rewrite ξ_t as:

$$\xi_t = c_1 \sigma_{\xi,t} \varepsilon^*_{\pi,t} + c_2 \sigma_{\xi,t} \varepsilon^*_{y,t} + c_3 \sigma_{\xi,t} \varepsilon^*_{l,t} + \xi^*_t, \xi^*_t \sim N\left(0, \left(1 - c^2_1 - c^2_2 - c^2_3\right) \sigma^2_{\xi,t}\right).$$

We can now rewrite the model in Eq. (11) as:

$$\begin{aligned} i_{t+1} =& \omega_{0,t} + \omega_{y,t}\left(y^{2\kappa_y - 1}_{t+1} + \frac{\gamma_y}{2} y^{3\kappa_y - 1}_{t+1}\right) + \omega_{l,t}\left(l^{2\kappa_l - 1}_{t+1} + \frac{\gamma_l}{2} l^{3\kappa_l - 1}_{t+1}\right) \\ &+ \omega_{\pi,t}\left(\left(\pi_{t+1} - \pi^*_{t+1}\right)^{2\kappa_\pi - 1} + \frac{\gamma_\pi}{2}\left(\pi_{t+1} - \pi^*_{t+1}\right)^{3\kappa_\pi - 1}\right) + \frac{1}{1 + e^{-\tilde{\varrho}_t}} i_t \\ &+ c_1 \sigma_{\xi,t} \varepsilon^*_{\pi,t} + c_2 \sigma_{\xi,t} \varepsilon^*_{y,t} + c_3 \sigma_{\xi,t} \varepsilon^*_{l,t} + \xi^*_t, \xi^*_t \sim N\left(0, \left(1 - c^2_1 - c^2_2 - c^2_3\right) \sigma^2_{\xi,t}\right). \end{aligned} \tag{19}$$

To address the nonlinearity in Eq. (19), we employ Taylor expansion. Denoting:

$$f\left(t; \tilde{\varrho}_t\right) = \frac{1}{1 + e^{-\tilde{\varrho}_t}} i_t,$$

and expanding around $\tilde{\varrho}_t = \tilde{\varrho}_{t|t} = \mathbb{E}_t\left(\tilde{\varrho}_t\right)$, we obtain:

$$f\left(t; \tilde{\varrho}_t\right) = f\left(t; \tilde{\varrho}_{t|t}\right) + \frac{\partial f\left(t; \tilde{\varrho}_t\right)}{\partial \tilde{\varrho}_t}\left(\tilde{\varrho}_t - \tilde{\varrho}_{t|t}\right).$$

This transformation yields a linear form:

$$Y_t = \boldsymbol{X}'_t \boldsymbol{\beta}_t + c_1 \sigma_{\xi,t} \varepsilon^*_{\pi,t} + c_2 \sigma_{\xi,t} \varepsilon^*_{y,t} + c_3 \sigma_{\xi,t} \varepsilon^*_{l,t} + \xi^*_t,$$

where:

$$Y_t = i_{t+1} - \frac{i_t}{1 + e^{-\tilde{\varrho}_{t|t}}} + \frac{i_t}{\left(1 + e^{-\tilde{\varrho}_{t|t}}\right)^2} e^{-\tilde{\varrho}_{t|t}} \tilde{\varrho}_{t|t},$$

Table 1
Estimation procedure for time-varying parameter monetary policy model.

Stage 1: Initialization of κ and γ
At this stage, we assign the value of κ (ranging from 0 to 3) and initialize γ. 1. Assign integer value to κ (ranging from 0 to 3) to define the functional form of the model specification. 2. Set initial value for γ at zero or leave it unspecified for subsequent estimation.
Stage 2: Instrumental variable estimation
For each target variable ($\pi_{t+1} - \pi^*_{t+1}$, y_{t+1}, l_{t+1}): 1. Specify the model: Variable$_{t+1} = Z_t\phi_t + \varepsilon_t$. 2. Determine the GARCH process: $\varepsilon_t \sim N\left(0, \sigma^2_{\varepsilon,\pi,t}\right)$, where $\sigma^2_{\varepsilon,t} = a_0 + a_1\sigma^2_{\varepsilon,t-1} + a_2\varepsilon^2_{t-1}$. 3. Define instrumental variables Z_t using lagged values of i_t, $\pi_t - \pi^*_t$, y_t, l_t, and $m2_t$. 4. Estimate time-varying parameters ϕ_t via Kalman filter. 5. Extract standardized prediction errors ε^*_t.
Stage 3: Addressing endogeneity
Decompose the error term ξ_t as a function of standardized prediction errors: $\xi_t = c_1\sigma_{\xi,t}\varepsilon^*_{\pi,t} + c_2\sigma_{\xi,t}\varepsilon^*_{y,t} + c_3\sigma_{\xi,t}\varepsilon^*_{l,t} + \xi^*_t, \xi^*_t \sim N\left(0, \left(1 - c_1^2 - c_2^2 - c_3^2\right)\sigma^2_{\xi,t}\right)$
Stage 4: Linearization via Taylor expansion
For the nonlinear smoothing term $f(t;\tilde{\varrho}_t) = \frac{1}{1+e^{-\tilde{\varrho}_t}} i_t$: 1. Apply first-order Taylor expansion around $\tilde{\varrho}_{t\|t} = \mathbb{E}_t(\tilde{\varrho}_t)$. 2. Transform the model into linear form: $Y_t = \boldsymbol{X}'_t\beta_t + \xi_t$
Stage 5: State-Space representation
Express the model in state-space form: 1. Measurement equation: $Y_t = \tilde{\boldsymbol{X}}'_t\tilde{\boldsymbol{\beta}}_t + c_1\sigma_{\xi,t}\varepsilon^*_{\pi,t} + c_2\sigma_{\xi,t}\varepsilon^*_{y,t} + c_3\sigma_{\xi,t}\varepsilon^*_{l,t} + \xi^*_t$. 2. State equation: $\tilde{\boldsymbol{\beta}}_t = G\tilde{\boldsymbol{\beta}}_{t-1} + \tilde{\varpi}_t$. 3. GARCH process: $\sigma^2_{\xi,t} = \alpha_0 + \alpha_1\xi^2_{t-1} + \alpha_2\sigma^2_{\xi,t-1}$.
Stage 6: Maximum likelihood estimation
Estimate parameters $\boldsymbol{\Theta}$ via maximum likelihood: 1. Implement Kalman filter to evaluate the likelihood function. 2. Maximize the likelihood to obtain parameter estimates. 3. Extract time-varying parameters $\boldsymbol{\beta}_t$ and other model components.

$$\boldsymbol{X}_t = \begin{pmatrix} 1 \\ y_{t+1}^{2\kappa_y-1} + \frac{\gamma_y}{2} y_{t+1}^{3\kappa_y-1} \\ l_{t+1}^{2\kappa_l-1} + \frac{\gamma_l}{2} l_{t+1}^{3\kappa_l-1} \\ \left(\pi_{t+1} - \pi^*_{t+1}\right)^{2\kappa_\pi-1} + \frac{\gamma_\pi}{2}\left(\pi_{t+1} - \pi^*_{t+1}\right)^{3\kappa_\pi-1} \\ \frac{i_{t-1}}{\left(1+e^{-\tilde{\varrho}_{t|t}}\right)^2} e^{-\tilde{\varrho}_{t|t}} \end{pmatrix}.$$

The model can now be expressed in state-space form:

$$Y_t = \tilde{\boldsymbol{X}}'_t\tilde{\boldsymbol{\beta}}_t + c_1\sigma_{\xi,t}\varepsilon^*_{\pi,t} + c_2\sigma_{\xi,t}\varepsilon^*_{y,t} + c_3\sigma_{\xi,t}\varepsilon^*_{l,t} + \xi^*_t, \xi^*_t \sim N\left(0, \left(1 - c_1^2 - c_2^2 - c_3^2\right)\sigma^2_{\xi,t}\right) \tag{20}$$

$$\tilde{\boldsymbol{\beta}}_t = G\tilde{\boldsymbol{\beta}}_{t-1} + \tilde{\varpi}_t, \tag{21}$$

$$\sigma^2_{\xi,t} = \alpha_0 + \alpha_1\xi^2_{t-1} + \alpha_2\sigma^2_{\xi,t-1}, \tag{22}$$

where $\tilde{\boldsymbol{X}}_t = \left(\boldsymbol{X}'_t, 1\right)'$, $\tilde{\boldsymbol{\beta}}_t = \left(\boldsymbol{\beta}'_t, \xi^*_t\right)'$, $G = \begin{pmatrix} I_5 & 0 \\ 0 & 0 \end{pmatrix}$, $\tilde{\varpi}_t = \left(\varpi'_t, \xi^*_t\right)'$,

$$\tilde{\varpi}_t \sim N\left(\mathbf{0}, \begin{pmatrix} \boldsymbol{\Sigma} & 0 \\ 0 & \left(1-\rho^2\right)\sigma^2_{e,t} \end{pmatrix}\right),$$

where $\Sigma = diag\left(\sigma_0^2, \sigma_y^2, \sigma_l^2, \sigma_\pi^2, \sigma_o^2\right)$.

After addressing endogeneity, the parameters to be estimated are

$$\boldsymbol{\Theta} = \left(\alpha_0, \alpha_1, \alpha_2, \gamma_\pi, \gamma_y, \gamma_l, \sigma_0^2, \sigma_y^2, \sigma_l^2, \sigma_\pi^2, \sigma_o^2, c_1, c_2, c_3\right)'.$$

The model specified in Eqs. (20)–(22) can be estimated using maximum likelihood estimation implemented through the Kalman filter. For clarity, we summarize the complete estimation procedure in Table 1.

Table 2
Model selection procedure.

Steps for optimal model identification
1. Estimate all 64 model specifications with varying κ and γ parameters.
2. For each model specification:
(a) Apply the six-stage estimation procedure outlined in Table 1.
(b) Obtain likelihood value $L\left(Data\middle\vert \boldsymbol{\Theta}, M_p\right)$ from the Kalman filter.
(c) Calculate AIC $= -2\ln L\left(Data\middle\vert \boldsymbol{\Theta}, M_p\right) + 2k$.
3. Select the model with the lowest AIC value as the optimal model.

3.2. Model selection

We conduct a comprehensive examination of the People's Bank of China's (PBoC) preferences, focusing on potential asymmetries and zone-like characteristics. We evaluate all possible model specifications presented in Table 4, encompassing 64 distinct models. We pre-specify integer values for the κ parameters ranging from 0 to 3 and estimate the remaining parameters as described in Section 3.1.

Since no general model specification permits nesting among the 64 models under consideration, conventional approaches such as the F-test or likelihood ratio test cannot be applied to identify the optimal specification. Following Riboni and Ruge-Murcia (2023), we utilize the Akaike Information Criterion (AIC) to select the model that best captures the underlying preference. This approach illuminates the nuances of the PBoC's preferences and enhances our understanding of their economic implications. The AIC is calculated as:

$$AIC = -2\ln L\left(Data\middle\vert \boldsymbol{\Theta}, M_p\right) + 2k \tag{23}$$

where $L\left(Data\middle\vert \boldsymbol{\Theta}, M_p\right)$ represents the likelihood for model p, obtained as a by-product of the Kalman filter, and k denotes the number of parameters in the model. The model with the lowest AIC value is selected, as it represents the optimal balance between model complexity and goodness of fit. The pseudocode for model selection is provided in Table 2.

4. Data

The dataset covers the period from 1996Q1 to 2022Q4. Each variable was processed using specific filtering methods and sourced from various data repositories:

(i) Nominal interest rate i_t: We use the quarterly interbank lending rate as a proxy for the nominal interest rate. This choice is based on the interbank lending rate's large market volume, high transaction share, and stability, which make it a more precise indicator of the cost of funds than the repo rate. The quarterly rate is derived by averaging the monthly interbank lending rates over a three-month period. The data is obtained from the official website of the People's Bank of China.[3]

(ii) Inflation gap $\pi_t - \pi_t^*$: We use the monthly Consumer Price Index (CPI) for China, sourced from the National Bureau of Statistics, as a proxy for inflation. The CPI is selected due to its strong connection to everyday life and its interpretability compared to other indices such as the Producer Price Index (PPI) or the GDP deflator. The inflation gap is calculated by subtracting the inflation target rate from the actual inflation rate. For the inflation target rate, we rely on the figure published in the report by the Premier of the State Council, which is widely recognized as an authoritative measure.

(iii) Output gap y_t: The output gap proxy is derived from quarterly GDP data. We calculate real GDP using the GDP levels and their cumulative real growth rates, then apply seasonal adjustments to these figures. The output gap is obtained through Hodrick–Prescott (HP) filtering of the seasonally adjusted real GDP.[4]

(iv) Credit leverage gap l_t: The Credit-to-GDP gap, commonly referred to as the Basel III countercyclical capital buffer indicator, measures the deviation of the credit-to-GDP ratio from its long-term trend, typically estimated using the Hodrick–Prescott (HP) filter. The credit leverage gap serves as a proxy for systemic risk and has become a focal point in the central bank's monetary policy objectives for two primary reasons. First, as leverage levels in China have escalated, the central bank has shifted emphasis from traditional goals such as economic growth and inflation toward addressing financial risk and leverage to mitigate systemic risks. Second, recent studies (Chen & Dai, 2018; Dong et al., 2021) suggest that China's monetary policy has increasingly prioritized leverage targets. We therefore incorporate the credit leverage gap in the monetary policy rule, reflecting its growing importance.

(v) The growth of $M2$: The growth of $M2$ is measured as the difference between two subsequent values of $M2$.

[3] Although the 7-day reverse repo rate has gained prominence as a primary policy tool in recent years (see Kim & Chen, 2022), we use the interbank lending rate as our policy rate measure given its stability and broad representation of monetary policy stance across our historical sample period.

[4] We employ a bilateral HP filter to construct historical output gap series for our ex-post analysis of central bank policy preferences. While this creates a potential mismatch between the two-sided filter and one-sided estimation procedure, we believe this approach remains appropriate for analyzing structural relationships in historical data. Our two-step methodology first uses the bilateral HP filter, the standard method for decomposing historical economic cycles, then applies the resulting series as input for our time-varying parameter model.

Table 3
The parameters estimated under the linear and selected models.

	Selected model ($\kappa_\pi = 3, \kappa_y = 1$)		Linear model	
	Estimates	Standard error	Estimates	Standard error
α_0	5.6392×10^{-11}	3.0542×10^{-11}	1.1566×10^{-8}	1.8806×10^{-7}
α_1	0.7507	7.5155×10^{-2}	0.8992	3.4761×10^{-2}
α_2	0.2493	7.5155×10^{-2}	0.1008	3.4761×10^{-2}
σ_0	3.5193×10^{-3}	2.8056×10^{-2}	1.7697×10^{-6}	1.0029×10^{-2}
σ_y	2.6417×10^{-2}	1.6235×10^{-2}	1.2939×10^{-2}	7.4667×10^{-3}
σ_l	7.8855×10^{-4}	9.6940×10^{-4}	2.0321×10^{-7}	2.4484×10^{-4}
σ_π	8.0680×10^{-5}	3.3797×10^{-5}	1.0522×10^{-6}	1.3071×10^{-3}
σ_o	1.8389×10^{-5}	7.6236×10^{-2}	8.9075×10^{-7}	1.3212×10^{-3}
γ_π	7.6789×10^{-3}	2.6123×10^{-4}	–	–
γ_y	0.2946	0.1437	–	–
c_1	-6.3396×10^{-3}	9.8953×10^{-2}	-7.5644×10^{-2}	0.1059
c_2	−0.1093	9.8245×10^{-2}	-4.1066×10^{-2}	9.7469×10^{-2}
c_3	-3.2330×10^{-2}	0.1027	-4.0574×10^{-2}	0.1068

5. Empirical results

In this section, we apply our proposed model and estimation strategy to explore the asymmetric and zone-like preferences of the PBoC. We estimate all 64 models based on the loss function forms outlined in Table 4. After obtaining the estimates, we compute AIC for each model and select the one that best captures the nuances of the PBoC's preferences. We focus specifically on comparing the chosen model with the linear benchmark model, where $\gamma_\pi = \gamma_l = \gamma_y = 0$ and $\kappa_\pi = \kappa_l = \kappa_y = 1$, to assess their relative performance.

5.1. Model selection and estimation

We estimate 64 models with time-varying parameters using the strategies outlined in Section 3.1. After completing model estimation, we calculate AIC values, as explained in Section 3.2. The AIC values are displayed in Fig. 2.

To visualize model performance, Panel (A) of Fig. 2 presents a 4×4 heatmap of AIC values. Each cell corresponds to a specific combination of κ and γ values for the output and leverage gaps, with $\kappa_\pi = 1$ and $\gamma_\pi \to 0$. Panels (B), (C), and (D) further explore the impact of κ_π by showing heatmaps for $\kappa_\pi = 1, 2$, and 3, respectively. In these panels, κ_y and κ_l are varied in the same manner as Panel (A).

Our analysis reveals two key findings. First, the AIC values across all models vary significantly, ranging from a maximum of 345.74 to a minimum of 149.95. Compared to the classic linear model (AIC = 157.52), the parameter combination of $\kappa_\pi = 3$, $\kappa_y = 1$, and $(\kappa_l = 1, \gamma_l \to 0)$ yields the lowest AIC value. Second, the loss function supported by AIC reveals pronounced nonlinearity. The corresponding loss functions, calculated without time-varying weights as per Eqs. (24)–(26), appear in Fig. 3. The figure indicates that the PBoC demonstrates asymmetric inertia in its response to the inflation gap, exhibits asymmetrical reactions to the output gap, and responds linearly to the leverage gap.

$$\text{Inflation gap: } \frac{1}{\kappa_\pi \gamma_\pi^2 \left(1-\rho_{t|t}\right)} \left[e^{\gamma_\pi \left(\pi_{t+1} - \pi^*_{t+1}\right)^{\kappa_\pi}} - \gamma_\pi \left(\pi_{t+1} - \pi^*_{t+1}\right)^{\kappa_\pi} - 1 \right], \tag{24}$$

$$\text{Output gap: } \frac{1}{\kappa_y \gamma_y^2} \left[e^{\gamma_y y_{t+1}^{\kappa_y}} - \gamma_y y_{t+1}^{\kappa_y} - 1 \right], \tag{25}$$

$$\text{Leverage gap: } l_{t+1}^2. \tag{26}$$

Table 3 presents the parameter estimates for the model selected based on AIC, with a comparison to the estimated linear monetary policy rule. The results reveal three key insights. First, both models show significant heteroscedasticity, as evidenced by the statistically significant GARCH(1,1) parameters. Second, the standard deviation of the time evolution of parameters varies between models. Third, the asymmetric parameters γ_π and γ_y are statistically significant and greater than zero, confirming asymmetric losses for inflation and the output gap. The next section will delve deeper into PBoC's preferences using the selected nonlinear model.

5.2. The time-varying characteristics of the central bank

In this section, we employ the Kalman filter to derive the time-varying parameters for both linear and selected nonlinear monetary policy rules. Using the estimation results presented in Table 3, we extract the time-varying parameters $\omega_{0,t}, \omega_{y,t}, \omega_{l,t}, \omega_{\pi,t}, \rho_t = \frac{1}{1+e^{-\varrho_t}}$, and ϱ_t for each period t, incorporating all available information up to that point. Fig. 4 illustrates the evolution of these parameters, offering insights into how the PBoC dynamically responds to the inflation gap, output gap, and leverage gap throughout the sample period. For comparative purposes, we also present the time-varying parameters within the framework of linear monetary policy.

Panel (A) of Fig. 4 shows that the trends of equilibrium interest rates, denoted as $\frac{\omega_{0,t|t}}{1-\rho_{t|t}}$, are remarkably similar under both linear and nonlinear monetary policy rules. The equilibrium interest rate in the selected nonlinear monetary policy is consistently lower

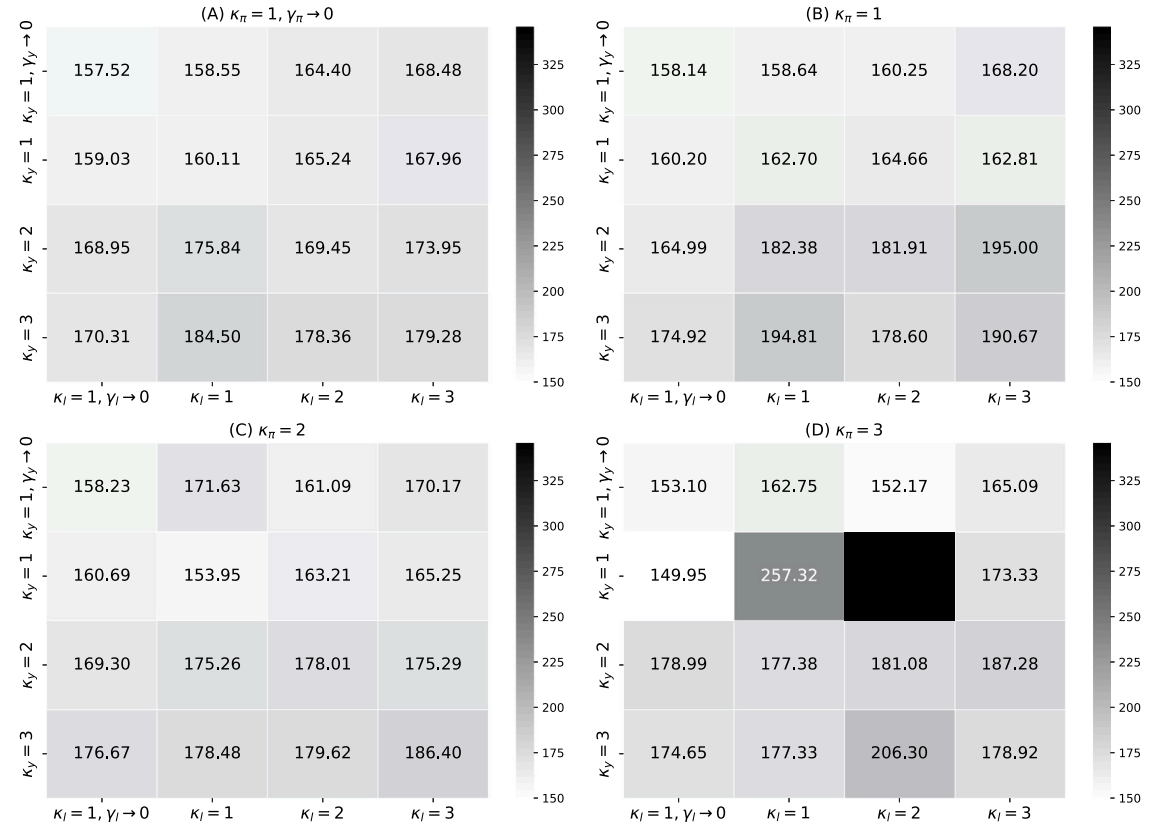

Fig. 2. The heatmaps of AIC of all model specifications.
Panel (A) presents a heatmap displaying a 4×4 matrix of AIC values for 16 combinations of $\kappa_y = 1, \gamma_y \to 0; \kappa_y = 1, 2, 3$ and $\kappa_I = 1, \gamma_I \to 0; \kappa_I = 1, 2, 3$, with $\kappa_\pi = 1$ and $\gamma_\pi \to 0$. Panels (B), (C), and (D) correspond to cases where κ_π equals 1, 2, and 3, respectively.

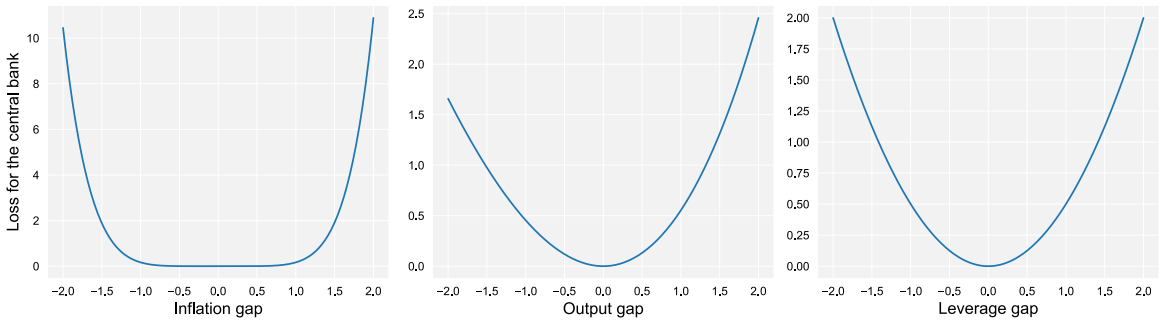

Fig. 3. The preference of the monetary authority in the selected model.

than that in the linear rules. The rate in the linear model demonstrates greater volatility compared to its nonlinear counterpart. The equilibrium interest rate serves as a fundamental benchmark for the PBoC's policy rate and plays a pivotal role in shaping monetary policy. From 2001 to 2008, a decline in the equilibrium interest rate suggests a shift toward looser monetary policies aimed at stimulating economic recovery. Beginning in 2008, the equilibrium interest rate started to rise. This upward trend has persisted since the Subprime Mortgage Crisis of 2008, reflecting an increased cost of financing in the market.

Panel (B) of Fig. 4 illustrates that the output gap coefficient is generally positive in both the linear and nonlinear model ($\kappa_y = 1, \gamma_y > 0$), indicating a counter-cyclical monetary policy approach by the PBoC. This implies that when there is a negative economic deviation, the PBoC adopts a stimulative policy by lowering interest rates. During a positive deviation, it tightens policy by raising interest rates. Prior to 2019, the coefficient was predominantly above zero, indicating the PBoC's preference to prevent an overheated economy rather than mitigate an economic downturn. However, a significant shift has occurred since 2020 as the coefficient turned negative, reflecting the impact of the COVID-19 pandemic on China's economy. This suggests that in the face

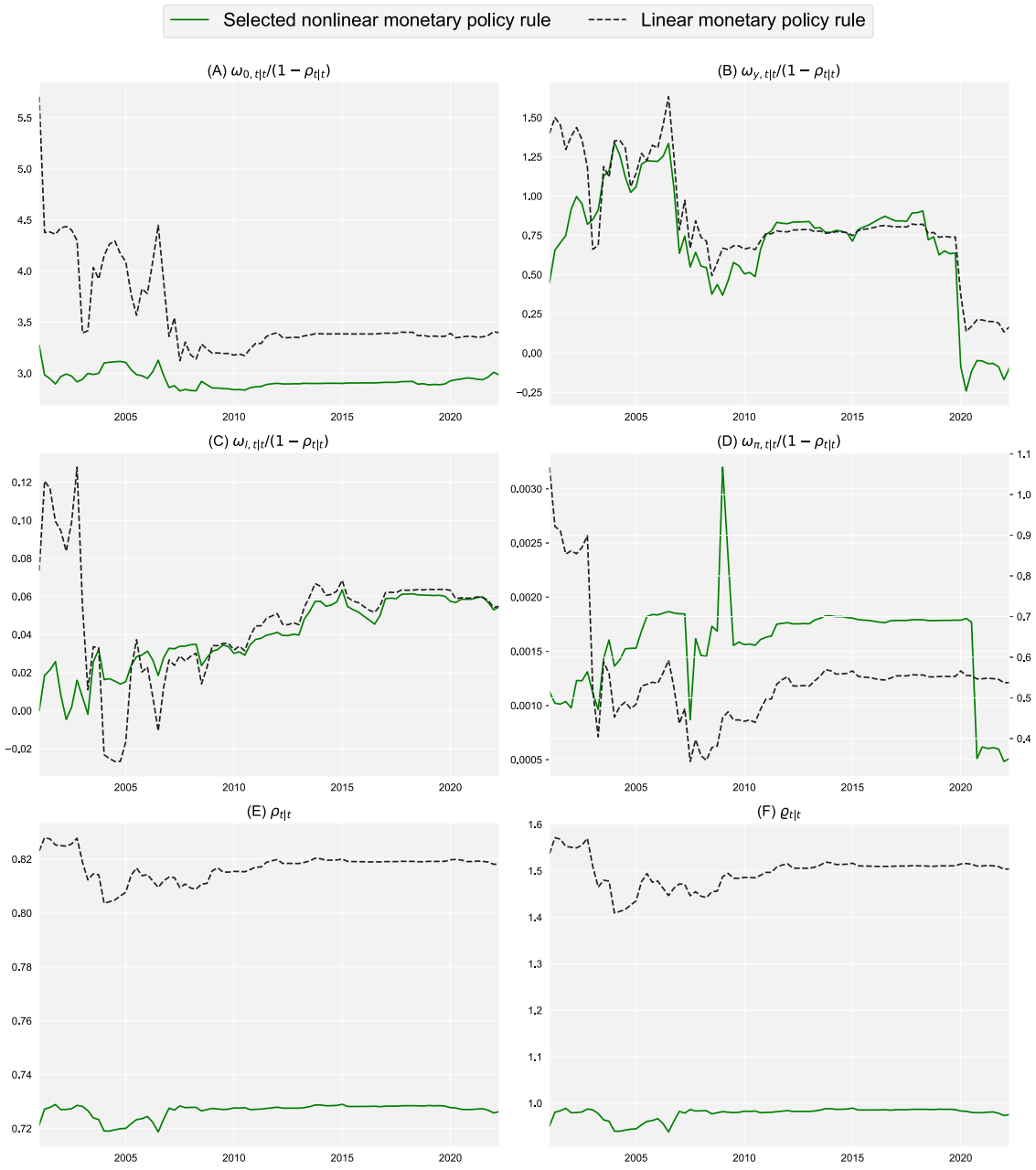

Fig. 4. Time-varying responses in linear and selected nonlinear monetary policy rules.
This figure displays the time-varying parameters $\frac{\omega_{0,t|t}}{1-\rho_{t|t}}$, $\frac{\omega_{y,t|t}}{1-\rho_{t|t}}$, $\frac{\omega_{l,t|t}}{1-\rho_{t|t}}$, $\frac{\omega_{\pi,t|t}}{1-\rho_{t|t}}$, $\rho_{t|t} = \frac{1}{1+e^{-\varrho_{t|t}}}$, and $\varrho_{t|t}$ estimated using the Kalman filter, as shown in Panels (A) to (F). The nonlinear model captures the monetary policy conduct. The notation "$t|t$" indicates the estimates obtained with data available up to time t. Panel (D) compares the nonlinear model (left axis) to the linear model (right axis).

of substantial negative external shocks, the central bank becomes more proactive in averting a recession. The dynamic nature of monetary policy underscores its adaptability in response to macroeconomic fluctuations. The transition from positive to negative values highlights a potential shift in China's macroeconomic policies from counter-cyclical to pro-cyclical regulation, aligning with prevailing economic conditions to maintain stable growth.

Panel (C) of Fig. 4 illustrates the evolution of credit leverage gap coefficients over time within both nonlinear and linear monetary policy frameworks. In the nonlinear model, these coefficients have generally increased, whereas in the linear model, they initially decreased before rising post-2008. The response to leverage gap in the nonlinear model ($\kappa_l = 1, \gamma_y \to 0$) is the same as the linear one. Before 2005, the coefficients in the nonlinear framework were relatively small and occasionally negative, indicating a pro-cyclical regulatory stance by the People's Bank of China (PBoC). This approach can be attributed to the low levels of credit leverage in China

during this period, which diminished the need for counter-cyclical regulation. Conversely, the linear model exhibited significant volatility, with coefficients peaking at 13% in 2002Q4 and dropping to −2% in 2004Q3, continuing to fluctuate until 2007. From 2007 onwards, both models show a similar upward trend in response to the leverage gap. The increasing coefficients reflect the central bank's heightened focus on leverage regulation, adopting a more robust counter-cyclical approach due to the rising macro leverage ratio in China. Counter-cyclical regulation reached its peak at 6.34% in the nonlinear model and 6.85% in the linear model by 2015Q1, maintaining a relatively high level through 2022. This underscores the elevated leverage risk and the ongoing necessity for strong counter-cyclical measures. In summary, China's monetary policy demonstrates a strong capacity for timely adjustments in regulating the leverage cycle and responding to evolving economic conditions and requirements.

Panel (D) of Fig. 4 demonstrates that the estimates under both monetary policy rules are consistently positive. In the context of a linear monetary policy rule, these positive values suggest a counter-cyclical strategy by the central bank in managing inflation targets. Specifically, the PBoC adopts a tightening stance to mitigate risks when inflation rises, signaling an overheated economy, and eases policy when inflation declines. The coefficients decrease from a peak of 1.07 in 2001Q1 to 0.34 by 2007Q3. They then exhibit an upward trend, reaching 0.538 by 2020Q4. In the nonlinear monetary policy rule, the PBoC's loss function concerning the inflation gap ($\kappa_\pi = 3, \gamma_\pi > 0$) is non-quadratic. Therefore, the time-varying coefficient cannot straightforwardly represent the PBoC's response to the inflation gap. Nevertheless, we observe a sharp increase in the coefficients during 2009Q1, attributed to the financial crisis, followed by a significant decline in 2020Q4 due to the pandemic.

The examination of the interest rate smoothing coefficients provides valuable insights into the PBoC's monetary policy strategies over time. Panels (E) and (F) of Fig. 4 show that the trends in parameter estimates for both linear and nonlinear models are generally aligned, although the coefficients in the nonlinear model are significantly smaller than those in the linear model. With all coefficients in both models exceeding 0.7, it is clear that both nonlinear and linear monetary policy rules aim to maintain a steady course, resulting in relatively larger coefficients (scaled by $1-\varrho_{t|t}$) for inflation, output, and credit targets. In both models, the coefficients fluctuate prior to 2007. After 2007, the smoothing coefficients exhibit an upward trend, increasing slightly from 0.723 (0.812) to around 0.726 (0.828) in the nonlinear (linear) monetary policy rule. These temporal variations in smoothing coefficients over time reflect the central bank's strategies in response to changing economic conditions, underscoring its commitment to maintaining financial market stability while addressing economic crises and recoveries.

5.3. The time-varying losses and responses of the central bank

In the following analysis, we investigate the time-varying preferences of the monetary authority by estimating the approximate loss surface associated with different economic gaps over time. We interpret $\omega_{y,t}$, $\omega_{l,t}$, and $\omega_{\pi,t}$ in (8) as the relative weights assigned to the losses incurred from deviations from policy targets. Accordingly, we calculate the relative approximated losses due to inflation ($\kappa_\pi = 3$), output ($\kappa_y = 1$), and leverage ($\kappa_l = 0$, $\gamma_l \to 0$) gaps using the following expressions:

$$\text{Inflation gap: } \frac{\omega_{\pi,t|t}}{\kappa_\pi \gamma_\pi^2 \left(1-\rho_{t|t}\right)} \left[e^{\gamma_\pi \left(\pi_{t+1}-\pi^*_{t+1}\right)^{\kappa_\pi}} - \gamma_\pi \left(\pi_{t+1}-\pi^*_{t+1}\right)^{\kappa_\pi} - 1 \right],$$

$$\text{Output gap: } \frac{\omega_{y,t|t}}{\kappa_y \gamma_y^2 \left(1-\rho_{t|t}\right)} \left[e^{\gamma_y y_{t+1}^{\kappa_y}} - \gamma_y y_{t+1}^{\kappa_y} - 1 \right],$$

$$\text{Leverage gap: } \frac{\omega_{l,t|t}}{\left(1-\rho_{t|t}\right)} l_{t+1}^2,$$

which are summarized in Fig. 5. We also present the time-varying response of the PBoC to gaps in inflation, output, and leverage in Fig. 6, which are derived as:

$$\text{Inflation gap: } \frac{\omega_{\pi,t|t}}{1-\rho_{t|t}} \left[\left(\pi_{t+1}-\pi^*_{t+1}\right)^{2\kappa_\pi - 1} + \frac{\gamma_\pi}{2} \left(\pi_{t+1}-\pi^*_{t+1}\right)^{3\kappa_\pi - 1} \right],$$

$$\text{Output gap: } \frac{\omega_{y,t|t}}{1-\rho_{t|t}} \left(y_{t+1}^{2\kappa_y - 1} + \frac{\gamma_y}{2} y_{t+1}^{3\kappa_y - 1} \right),$$

$$\text{Leverage gap: } \frac{\omega_{l,t|t}}{1-\rho_{t|t}} l_{t+1}.$$

A closer examination of Figs. 5 and 6 reveals three significant observations.

First, the analysis of the loss function associated with the inflation gap reveals an apparent inertia with a slightly asymmetrical pattern, as illustrated in Figs. 3 and 5. These figures highlight the monetary authority's inertial approach to addressing inflation shocks. Specifically, the PBoC tends to refrain from intervention unless inflation deviates by more than 1% from the target, irrespective of the direction of this deviation. However, once the deviation surpasses 1%, the central bank engages in asymmetrical counter-cyclical regulation, suggesting an inertial zone within approximately a (−1%, 1%) deviation range for managing inflation through monetary policy. Furthermore, the PBoC exhibits a slightly greater aversion to high inflation levels compared to low inflation levels, indicated by $\gamma_\pi > 0$. The response to inflation gaps, depicted in Fig. 6, indicates that a 1% increase in inflation above the target results in an interest rate hike ranging from 0.05% to 0.3% over time. Conversely, a 1% decrease below the target leads to an interest rate reduction ranging from 0.04% to 0.3% over time. Importantly, due to the COVID-19 pandemic, the PBoC's counter-cyclical regulation has undergone significant changes and has become more moderate since 2020Q4. This pattern suggests that the PBoC's monetary policy response to inflation is relatively moderate. The presence of zone-like preferences indicates that the central bank maintains a clear policy boundary when regulating inflation.

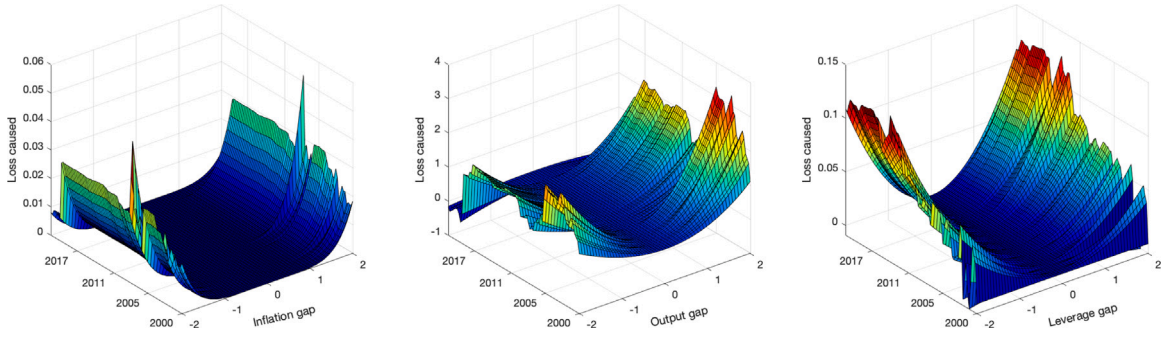

Fig. 5. The time-varying relative loss caused by inflation, output and leverage gaps.

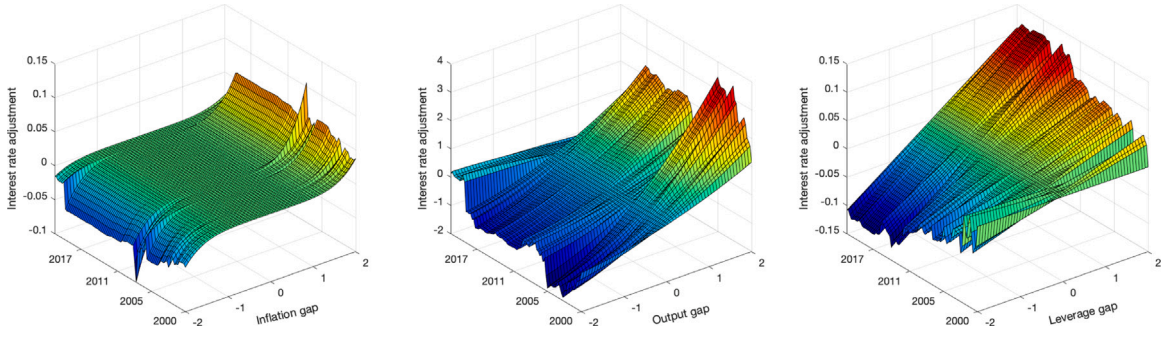

Fig. 6. The time-varying responses of monetary policy to inflation, output and leverage gaps.

Second, with respect to the output gap, the loss function of the PBoC exhibits an asymmetric characteristic, indicating a stronger aversion to economic overheating than to recession, as shown by Fig. 3. The time-varying relative weights, denoted by $\frac{\omega_{y,t|t}}{(1-\rho_{t|t})}$, reveal that the PBoC's losses have fluctuated and turned negative, indicating gains, since 2020Q1, primarily due to the impact of the COVID-19 pandemic. In alignment with these time-varying losses, the responses to the output gaps suggest that monetary policy followed an asymmetric counter-cyclical stance for managing output gaps until 2020Q1, after which it shifted to a pro-cyclical approach. Unlike inflation regulation, there is no "inertia zone" observed in this context. The regulatory force applied to mitigate positive output gaps is stronger than that for negative gaps of equivalent magnitude, reflecting the asymmetry in the PBoC's loss function concerning the output gap. These findings imply that China has prioritized maintaining stable economic growth over strict economic cycle regulation.

Third, for the leverage gaps, the PBoC employs a symmetrical regulatory approach in the absence of inertia. This implies that the central bank intervenes with equal intensity regardless of whether the leverage level deviates upward or downward. As shown in Figs. 5 and 6, earlier monetary policies did not explicitly show a regulatory stance for leverage targets. This observation is consistent with empirical findings indicating that prior to 2005, both time-varying losses and policy responses were minimal and occasionally reversed direction. However, from 2005 onwards, there has been a noticeable increase in relative weights, $\frac{\omega_{l,t|t}}{(1-\rho_{t|t})}$, reflecting a stronger focus on mitigating excessive credit growth. During this period, the PBoC implements a counter-cyclical framework. Consequently, the time-varying losses associated with the leverage gap have increased, as Fig. 5 depicts. The intensity of policy interventions has also risen over time, which is indicated by Fig. 6.

5.4. Robustness

We conduct robustness checks by comparing our proposed model specifications against two alternatives: models with constant parameters and time-varying parameter models that exclude leverage gaps. Figs. 7 and 8 present the AIC values for all model specifications. The results clearly indicate that AIC values for these alternative models consistently exceed those of our selected nonlinear monetary policy model discussed in previous sections.

The lowest AIC value for the constant parameter model is 154.95, while the lowest AIC value for the time-varying parameter models without leverage gaps is 153.31. These findings provide strong evidence that our proposed nonlinear policy model offers superior fit, as it achieves a lower AIC value relative to all considered alternatives.

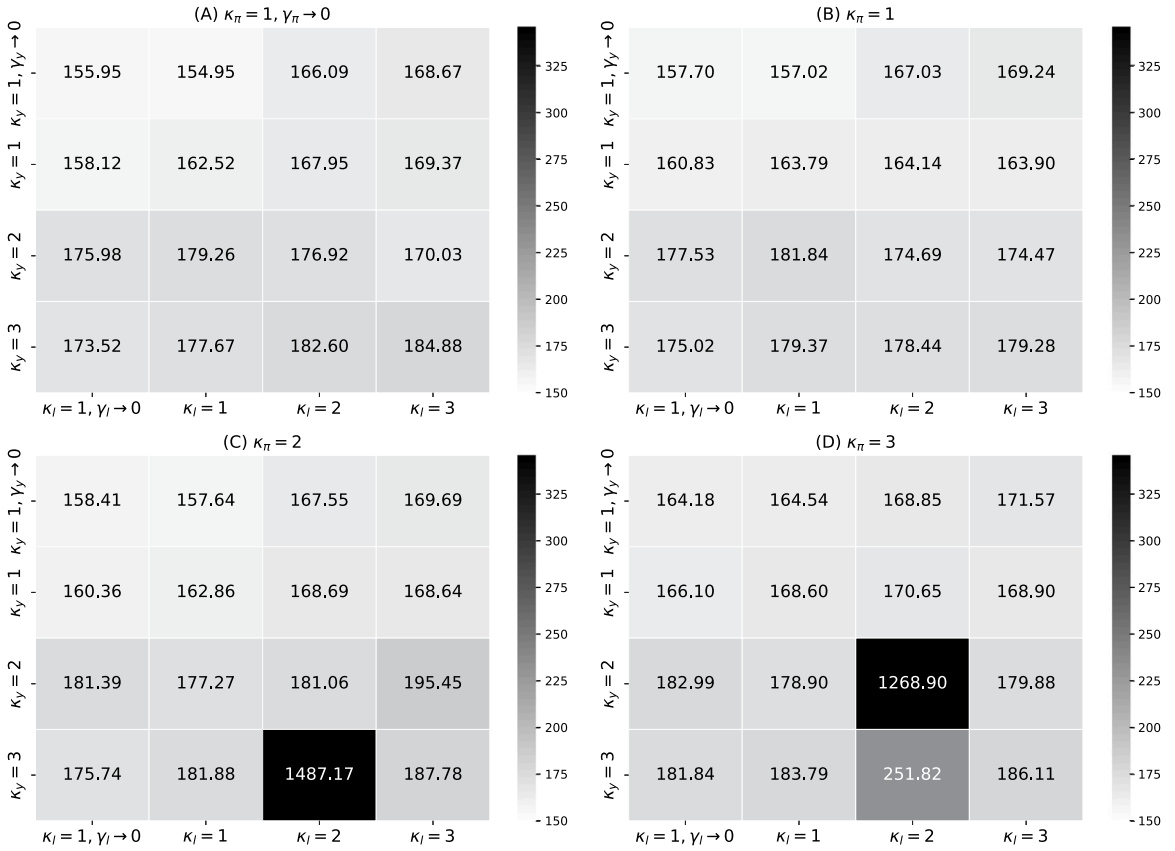

Fig. 7. The heatmaps of AIC of all model specifications with constant parameters.
Panel (A) presents a heatmap displaying a 4 × 4 matrix of AIC for 16 combinations of $\kappa_y = 1, \gamma_y \to 0; \kappa_y = 1, 2, 3$ and $\kappa_l = 1, \gamma_l \to 0; \kappa_l = 1, 2, 3$, with $\kappa_\pi = 1$ and $\gamma_\pi \to 0$. Panels (B), (C), and (D) correspond to cases where κ_π equals 1, 2, and 3, respectively.

6. Conclusion

This paper proposes a new framework for analyzing the time-varying asymmetric and zone-like preferences in the monetary policy response function of central banks. Using this framework, we examine the characteristics embedded in the preference of the People's Bank of China (PBoC). We hypothesize that the relative importance assigned to different policy objectives in the PBoC's loss function evolves temporally. Under this premise, the central bank formulates an optimal forward-looking monetary policy rule with time-varying parameters by minimizing its dynamic losses.

Our analysis considers four distinct types of losses related to inflation, output, and leverage, generating 64 unique model specifications. We extend conventional maximum likelihood estimation techniques to accommodate these models and employ the Akaike information criterion (AIC) to identify the most appropriate specification. We validate our selected model by comparing it against time-varying parameter models that exclude leverage targets and models with constant parameters. AIC analysis confirms that our proposed model provides the best fit, reinforcing its analytical robustness.

Examination of time-varying policy reactions reveals three key insights into the PBoC's monetary policy framework. First, the central bank employs an inertial approach to managing inflation gaps, intervening only when inflation deviates by more than 1% from its target. Within this "inert zone" (−1%, 1%), the PBoC refrains from intervention, allowing market mechanisms to operate. The central bank demonstrates slightly greater concern for inflation overshooting than undershooting. When inflation exceeds its target by 1%, the PBoC typically raises interest rates by 0.05% to 0.3%, while a 1% decrease below target triggers a reduction of 0.04% to 0.3%. Since late 2020, influenced by COVID-19, the PBoC's counter-cyclical measures have become more moderate, reflecting a cautious monetary policy approach with clearly defined intervention boundaries for inflation management.

Second, the PBoC exhibits stronger aversion to economic overheating than to recession. Since early 2020, due to the COVID-19 pandemic, the PBoC's losses have fluctuated, occasionally transforming into gains. Before 2020, monetary policy operated counter-cyclically but subsequently shifted to a pro-cyclical orientation. Unlike its approach to inflation, the PBoC maintains no "inertia zone" for output gaps. The central bank applies greater regulatory pressure to contain positive output gaps than to address negative gaps of equal magnitude, underscoring its asymmetric loss function. This policy stance suggests that China prioritizes stable economic growth over strict cyclical regulation.

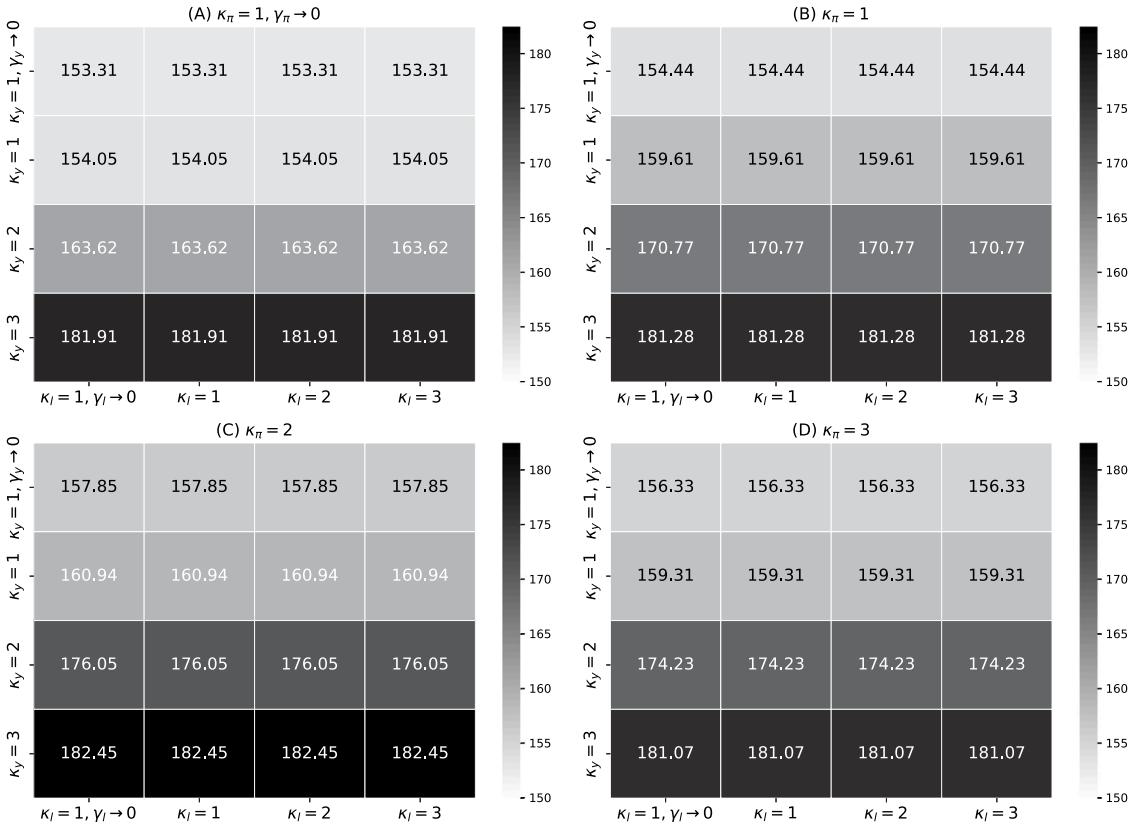

Fig. 8. The heatmaps of AIC of all model specifications without leverage gaps.
Panel (A) presents a heatmap displaying a 4×4 matrix of AIC for 16 combinations of $\kappa_y = 1, \gamma_y \to 0; \kappa_y = 1, 2, 3$ and $\kappa_l = 1, \gamma_l \to 0; \kappa_l = 1, 2, 3$, with $\kappa_\pi = 1$ and $\gamma_\pi \to 0$. Panels (B), (C), and (D) correspond to cases where κ_π equals 1, 2, and 3, respectively.

Third, the PBoC implements a symmetric regulatory approach to leverage gaps, responding with equal intensity regardless of whether leverage levels rise or fall. Prior to 2005, monetary policies did not explicitly target leverage, with minimal and occasionally contradictory responses. Since then, a pronounced shift toward controlling credit growth has emerged, evidenced by heightened policy focus and intervention intensity. This strategic evolution is reflected in increasing time-varying losses and more decisive policy measures targeting leverage.

Our empirical findings and analysis highlight the flexibility and analytical power of our modeling framework. This study illuminates the dynamic nature of the PBoC's monetary policy approach, emphasizing its evolving priorities and strategic adaptability across varying economic conditions.

Appendix A. Different specifications for the loss function

See Table 4.

Appendix B. The derivation of the optimal interest rate for the central bank

The FOCs in Eq. (5) can be derived as below. First, we can find that

$$\begin{aligned}\frac{\partial L_t}{\partial i_t} =& t\tilde{w}_{i,t}\left(i_t - i_t^*\right) \\ &- \mathcal{G}\left(\pi_t - \pi_t^*; \kappa_\pi, \gamma_\pi\right)\left(\pi_t - \pi_t^*\right)\lambda\theta_1 \\ &- t\tilde{w}_{y,t}\mathcal{G}\left(y_t; \kappa_y, \gamma_y\right) y_t\theta_1 \\ &- t\tilde{w}_{l,t}\mathcal{G}\left(l_t; \kappa_l, \gamma_l\right) l_t\left(k_1 + \theta_1 k_2\right) \\ \frac{\partial L_{t+\tau}}{\partial i_t} =& 0, \text{ for } \tau \geq 1.\end{aligned}$$

Table 4
Specifications of the loss function on inflation gap, output gap and leverage gap
The specifications of the preference toward output gap (I), leverage gap (II) and inflation gap (III) given different sets of parameters.

		$\kappa_\pi = 1, \gamma_\pi \to 0$	$\kappa_\pi = 1$	$\kappa_\pi = 2$	$\kappa_\pi = 3$
$\kappa_y = 1$ $\gamma_y \to 0$	$\kappa_l = 1$ $\gamma_l \to 0$	I: Quadratic II: Quadratic III: Quadratic	I: Quadratic II: Quadratic III: Asymmetric	I: Quadratic II: Quadratic III: Symmetrically inert	I: Quadratic II: Quadratic III: Asymmetrically inert
	$\kappa_l = 1$	I: Quadratic II: Asymmetric III: Quadratic	I: Quadratic II: Asymmetric III: Asymmetric	I: Quadratic II: Asymmetric III: Symmetrically inert	I: Quadratic II: Asymmetric III: Asymmetrically inert
	$\kappa_l = 2$	I: Quadratic II: Symmetrically inert III: Quadratic	I: Quadratic II: Symmetrically inert III: Asymmetric	I: Quadratic II: Symmetrically inert III: Symmetrically inert	I: Quadratic II: Symmetrically inert III: Asymmetrically inert
	$\kappa_l = 3$	I: Quadratic II: Asymmetrically inert III: Quadratic	I: Quadratic II: Asymmetrically inert III: Asymmetric	I: Quadratic II: Asymmetrically inert III: Symmetrically inert	I: Quadratic II: Asymmetrically inert III: Asymmetrically inert
$\kappa_y = 1$	$\kappa_l = 1$ $\gamma_l \to 0$	I: Asymmetric II: Quadratic III: Quadratic	I: Asymmetric II: Quadratic III: Asymmetric	I: Asymmetric II: Quadratic III: Symmetrically inert	I: Asymmetric II: Quadratic III: Asymmetrically inert
	$\kappa_l = 1$	I: Asymmetric II: Asymmetric III: Quadratic	I: Asymmetric II: Asymmetric III: Asymmetric	I: Asymmetric II: Asymmetric III: Symmetrically inert	I: Asymmetric II: Asymmetric III: Asymmetrically inert
	$\kappa_l = 2$	I: Asymmetric II: Symmetrically inert III: Quadratic	I: Asymmetric II: Symmetrically inert III: Asymmetric	I: Asymmetric II: Symmetrically inert III: Symmetrically inert	I: Asymmetric II: Symmetrically inert III: Asymmetrically inert
	$\kappa_l = 3$	I: Asymmetric II: Asymmetrically inert III: Quadratic	I: Asymmetric II: Asymmetrically inert III: Asymmetric	I: Asymmetric II: Asymmetrically inert III: Symmetrically inert	I: Asymmetric II: Asymmetrically inert III: Asymmetrically inert
$\kappa_y = 2$	$\kappa_l = 1$ $\gamma_l \to 0$	I: Symmetrically inert II: Quadratic III: Quadratic	I: Symmetrically inert II: Quadratic III: Asymmetric	I: Symmetrically inert II: Quadratic III: Symmetrically inert	I: Symmetrically inert II: Quadratic III: Asymmetrically inert
	κ_l=1	I: Symmetrically inert II: Asymmetric III: Quadratic	I: Symmetrically inert II: Asymmetric III: Asymmetric	I: Symmetrically inert II: Asymmetric III: Symmetrically inert	I: Symmetrically inert II: Asymmetric III: Asymmetrically inert
	$\kappa_l = 2$	I: Symmetrically inert II: Symmetrically inert III: Quadratic	I: Symmetrically inert II: Symmetrically inert III: Asymmetric	I: Symmetrically inert II: Symmetrically inert III: Symmetrically inert	I: Symmetrically inert II: Symmetrically inert III: Asymmetrically inert
	$\kappa_l = 3$	I: Symmetrically inert II: Asymmetrically inert III: Quadratic	I: Symmetrically inert II: Asymmetrically inert III: Asymmetric	I: Symmetrically inert II: Asymmetrically inert III: Symmetrically inert	I: Symmetrically inert II: Asymmetrically inert III: Asymmetrically inert
$\kappa_y = 3$	$\kappa_l = 1$ $\gamma_l \to 0$	I: Asymmetrically inert II: Quadratic III: Quadratic	I: Asymmetrically inert II: Quadratic III: Asymmetric	I: Asymmetrically inert II: Quadratic III: Symmetrically inert	I: Asymmetrically inert II: Quadratic III: Asymmetrically inert
	κ_l=1	I: Asymmetrically inert II: Asymmetric III: Quadratic	I: Asymmetrically inert II: Asymmetric III: Asymmetric	I: Asymmetrically inert II: Asymmetric III: Symmetrically inert	I: Asymmetrically inert II: Asymmetric III: Asymmetrically inert
	$\kappa_l = 2$	I: Asymmetrically inert II: Symmetrically inert III: Quadratic	I: Asymmetrically inert II: Symmetrically inert III: Asymmetric	I: Asymmetrically inert II: Symmetrically inert III: Symmetrically inert	I: Asymmetrically inert II: Symmetrically inert III: Asymmetrically inert
	$\kappa_l = 3$	I: Asymmetrically inert II: Asymmetrically inert III: Quadratic	I: Asymmetrically inert II: Asymmetrically inert III: Asymmetric	I: Asymmetrically inert II: Asymmetrically inert III: Symmetrically inert	I: Asymmetrically inert II: Asymmetrically inert III: Asymmetrically inert

where $\mathcal{G}(x;\kappa,\gamma) = \frac{x^{\kappa-2}\left(e^{\gamma x^{\kappa}}-1\right)}{\gamma}$. Therefore,

$$\begin{aligned}
&\mathbb{E}_{t-1}\left[\frac{\partial L_t}{\partial i_t} + \sum_{\tau=1}\delta^{\tau}\frac{\partial L_{t+\tau}}{\partial i_t}\right] \\
&= -\theta_1\mathbb{E}_{t-1}\left[\tilde{w}_{y,t}\mathcal{G}\left(y_t;\kappa_y,\gamma_y\right)y_t\right] - \left(k_1+\theta_1 k_2\right)\mathbb{E}_{t-1}\left[\tilde{w}_{l,t}\mathcal{G}\left(l_t;\kappa_l,\gamma_l\right)l_t\right] + \mathbb{E}_{t-1}\left[\tilde{w}_{i,t}\left(i_t - i_t^*\right)\right] \\
&\quad - \lambda\theta_1\mathbb{E}_{t-1}\left[\mathcal{G}\left(\pi_t-\pi_t^*;\kappa_\pi,\gamma_\pi\right)\left(\pi_t-\pi_t^*\right)\right] = 0,
\end{aligned}$$

and since $\tilde{w}_{y,t}$, $\tilde{w}_{l,t}$, and $\tilde{w}_{i,t}$ are relative and time-varying and independent of $\left(\pi_t-\pi_t^*\right)$, y_t and l_t, we have

$$\mathbb{E}_{t-1}\left[i_t\right] = \mathbb{E}_{t-1}\left[i_t^*\right] + \mathbb{E}_{t-1}\left[\frac{\tilde{w}_{y,t}\theta_1}{\tilde{w}_{i,t}}\right]\mathbb{E}_{t-1}\left[\mathcal{G}\left(y_t;\kappa_y,\gamma_y\right)y_t\right] + \mathbb{E}_{t-1}\left[\frac{\tilde{w}_{l,t}\left(k_1+\theta_1 k_2\right)}{\tilde{w}_{i,t}}\right]\mathbb{E}_{t-1}\left[\mathcal{G}\left(l_t;\kappa_l,\gamma_l\right)l_t\right]$$

$$+\ \mathbb{E}_{t-1}\left[\frac{\lambda\theta_1}{\tilde{w}_{i,t}}\right]\mathbb{E}_{t-1}\left[\mathcal{G}\left(\pi_t-\pi_t^*;\kappa_\pi,\gamma_\pi\right)\left(\pi_t-\pi_t^*\right)\right].$$

Let $\omega_{0,t}=\mathbb{E}_t\left[i_{t+1}^*\right]$, $\omega_{y,t}=\mathbb{E}_t\left[\frac{\tilde{w}_{y,t+1}\theta_1}{\tilde{w}_{i,t+1}}\right]$, $\omega_{l,t}=\mathbb{E}_t\left[\frac{\tilde{w}_{l,t+1}(k_1+\theta_1k_2)}{\tilde{w}_{i,t+1}}\right]$ $\omega_{\pi,t}=\mathbb{E}_t\left[\frac{\lambda\theta_1}{\tilde{w}_{i,t+1}}\right]$, and $\hat{i}_t=\mathbb{E}_t\left[i_{t+1}\right]$, we can have,

$$\begin{aligned}\hat{i}_t=&\omega_{0,t}+\omega_{y,t}\mathbb{E}_t\left[\mathcal{G}\left(y_{t+1};\kappa_y,\gamma_y\right)y_{t+1}\right]+\omega_{l,t}\mathbb{E}_t\left[\mathcal{G}\left(l_{t+1};\kappa_l,\gamma_l\right)l_{t+1}\right]\\&+\ \omega_{\pi,t}\mathbb{E}_t\left[\mathcal{G}\left(\pi_{t+1}-\pi_{t+1}^*;\kappa_\pi,\gamma_\pi\right)\left(\pi_{t+1}-\pi_{t+1}^*\right)\right].\end{aligned}$$

Data availability

Data will be made available on request.

References

Adrian, T., Boyarchenko, N., & Giannone, D. (2019). Vulnerable growth. *American Economic Review*, *109*(4), 1263–1289.

Auclert, A. (2019). Monetary policy and the redistribution channel. *American Economic Review*, *109*(6), 2333–2367.

Baele, L., Bekaert, G., Cho, S., Inghelbrecht, K., & Moreno, A. (2015). Macroeconomic regimes. *Journal of Monetary Economics*, *70*, 51–71.

Bartscher, A. K., Kuhn, M., Schularick, M., & Steins, U. (2020). Modigliani meets minsky: Inequality, debt, and financial fragility in america, 1950–2016. *SSRN Electronic Journal*.

Benigno, P., & Rossi, L. (2021). Asymmetries in monetary policy. *European Economic Review*, *140*, Article 103945.

Bianchi, F., Lettau, M., & Ludvigson, S. C. (2022). Monetary policy and asset valuation. *The Journal of Finance*, *77*(2), 967–1017.

Blanchard, O. (2019). Public debt and low interest rates. *American Economic Review*, *109*(4), 1197–1229.

Boinet, V., & Martin, C. (2008). Targets, zones, and asymmetries: a flexible nonlinear model of recent UK monetary policy. *Oxford Economic Papers*, *60*(3), 423–439.

Boivin, J. (2006). Has U.S. monetary policy changed? Evidence from drifting coefficients and real-time data. *Journal of Money Credit and Banking*, *38*, 1149–1173.

Borio, C. E., & Lowe, P. W. (2002). *Asset prices, financial and monetary stability: exploring the nexus, BIS Working Papers, vol. 114*.

Bruno, V., & Shin, H. S. (2015). Capital flows and the risk-taking channel of monetary policy. *Journal of Monetary Economics*, *71*, 119–132.

Castro, V. (2011). Can central banks' monetary policy be described by a linear (augmented) Taylor rule or by a nonlinear rule? *Journal of Financial Stability*, *7*(4), 228–246.

Chen, C., & Dai, M. (2018). Monetary policy, leverage cycle, and house price fluctuation. *Economic Research Journal*, *53*(9), 52–67.

Cogley, T., & Sargent, T. J. (2005). Drifts and volatilities: monetary policies and outcomes in the post WWII US. *Review of Economic Dynamics*, *8*(2), 262–302.

Dong, B., Xu, H., & Tan, X. (2021). Can monetary policy reconcile sustaining steady growth with preventing risks in China? An analysis based on dynamic stochastic general equilibrium modeling. *Journal of Financial Research*, *490*(4), 19–37.

Drehmann, M., & Tsatsaronis, K. (2014). The credit-to-GDP gap and countercyclical capital buffers: questions and answers. *BIS Quarterly Review March*.

Filardo, A., Hubert, P., & Rungcharoenkitkul, P. (2022). Monetary policy reaction function and the financial cycle. *Journal of Banking and Finance*, *142*, Article 106536.

Gambacorta, L., & Signoretti, F. M. (2014). Should monetary policy lean against the wind?: An analysis based on a DSGE model with banking. *Journal of Economic Dynamics & Control*, *43*, 146–174.

Giannoni, M. P., & Woodford, M. (2017). Optimal target criteria for stabilization policy. *Journal of Economic Theory*, *168*, 55–106.

Gourinchas, P.-O., & Rey, H. (2019). *Global real rates: A secular approach, BIS Working Paper*. No. 793, SSRN: https://ssrn.com/abstract=3420309.

Gross, I., & Hansen, J. (2021). Optimal policy design in nonlinear DSGE models: An n-order accurate approximation. *European Economic Review*, *140*, Article 103918.

Kim, S., & Chen, H. (2022). From a quantity to an interest rate-based framework: multiple monetary policy instruments and their effects in China. *Journal of Money Credit and Banking*, *54*(7), 2103–2123.

Kim, C.-J., & Nelson, C. R. (2006). Estimation of a forward-looking monetary policy rule: A time-varying parameter model using ex post data. *Journal of Monetary Economics*, *53*(8), 1949–1966.

Nakajima, J., & West, M. (2013). Bayesian analysis of latent threshold dynamic models. *Journal of Business & Economic Statistics*, *31*(2), 151–164.

Orphanides, A., & Wieland, V. (2000). Inflation zone targeting. *European Economic Review*, *44*(7), 1351–1387.

Primiceri, G. E. (2005). Time varying structural vector autoregressions and monetary policy. *Review of Economic Studies*, *72*(3), 821–852.

Riboni, A., & Ruge-Murcia, F. (2023). The power of the federal reserve chair. *International Economic Review*, *64*(2), 727–756.

Robert Nobay, A., & Peel, D. A. (2003). Optimal discretionary monetary policy in a model of asymmetric central bank preferences. *The Economic Journal*, *113*(489), 657–665.

Ruge-Murcia, F. J. (2003). Inflation targeting under asymmetric preferences. *Journal of Money Credit and Banking*, *35*(5), 763–785.

Shapiro, A. H., & Wilson, D. J. (2022). Taking the fed at its word: A new approach to estimating central bank objectives using text analysis. *Review of Economic Studies*, *89*(5), 2768–2805.

Silvo, A. (2019). The interaction of monetary and macroprudential policies. *Journal of Money Credit and Banking*, *51*(4), 859–894.

Sims, C. A., & Zha, T. (2001). *Stability and instability in US monetary policy behavior*. Princeton University.

Sims, C. A., & Zha, T. (2006). Were there regime switches in US monetary policy? *American Economic Review*, *96*(1), 54–81.

Surico, P. (2007). The Fed's monetary policy rule and US inflation: The case of asymmetric preferences. *Journal of Economic Dynamics & Control*, *31*(1), 305–324.

Taylor, J. B. (1993). Discretion versus policy rules in practice. *Vol. 39*, In *Carnegie-Rochester conference series on public policy* (pp. 195–214). Elsevier.

Woodford, M., & Walsh, C. E. (2005). Interest and prices: Foundations of a theory of monetary policy. *Macroeconomic Dynamics*, *9*(3), 462–468.